ELSEVIER

Journal of Organometallic Chemistry 648 (2002) 176–187

Journal of Organometallic Chemistry

www.elsevier.com/locate/jorganchem

Synthesis, characterization and crystal structures of alkyl-, alkynyl-, alkoxo- and halo-magnesium amides

Kuo-Ching Yang [a,b], Chung-Cheng Chang [c,*], Jyh-Yuan Huang [a], Chih-Chien Lin [a], Gene-Hsiang Lee [d], Yu Wang [d], Michael Y. Chiang [a]

[a] *Department of Chemistry, National Sun Yat-Sen University, Kaohsiung, Taiwan, ROC*
[b] *Department of Chemical Engineering, Chengshiu Institute of Technology, Kaohsiung, Taiwan, ROC*
[c] *Department of Applied Chemistry, National University of Kaohsiung, No. 251, Lane 280, Der-Chun Road, Kaohsiung 811, Taiwan, ROC*
[d] *Department of Chemistry, National Taiwan University, Taipei, Taiwan, ROC*

Received 23 August 2001; received in revised form 19 November 2001; accepted 20 November 2001

Abstract

In our experiments, 1:1 stoichiometric reaction between MgR_2 and diphenylamine produced the monomeric heteroleptic alkylmagnesium amides $[RMgNPh_2(THF)_2]$ [R = Et **1** and ^{i}Pr **2**]. Adding the stronger donor solvent HMPA (HMPA=hexamethylphosphoramide) to compound **1** caused disproportionation resulting in a bisamidomagnesium compound $[Mg(NPh_2)_2(HMPA)_2]$ **3**. The stoichiometric reaction between bis(diisopropylamido)-magnesium and different substituted acetylenes HC≡CR in THF solution produced two dimeric amidomagnesium acetylide compounds $[(RC{\equiv}C)Mg(\mu\text{-}N^iPr_2)(THF)]_2$ [R = Ph **4**, R = $SiMe_3$ **5**]. When the differently sized secondary amines, $HNEt_2$ and $HN(SiMe_3)_2$, were reacted with Grignard reagent EtMgBr, they produced diethylamino-bridging and bromo-bridging Hauser base $[BrMg(\mu\text{-}NEt_2)(HMPA)]_2$ **6** and $[(Me_3Si)_2NMg(\mu\text{-}Br)(OEt_2)]_2$ **7,** respectively. Unexpectedly, the reaction of $MgEt_2$ and $HN(SiMe_3)_2$ in refluxing THF produced $[(Me_3Si)_2NMg(\mu\text{-}OEt)(THF)]_2$ **8**. Additionally, we synthesized the first trinuclear magnesium compound $[(^tBuC{\equiv}C)(THF)Mg(\mu\text{-}C{\equiv}C^tBu)(\mu\text{-}N^iPr_2)Mg(\mu\text{-}C{\equiv}C^tBu)(\mu\text{-}N^iPr_2)Mg(THF)(C{\equiv}C^tBu)]$ **9**, which exhibited both an electron-rich bridging ligand N^iPr_2 and electron-deficient bridging ligand $C{\equiv}C^tBu$. All of these new compounds (**1**–**9**) were characterized by ^{1}H-, ^{13}C-, ^{31}P-NMR, IR spectroscopy, mass spectrometry and X-ray crystallography.

Keywords: Heteroleptic magnesium amides; Hauser base; Alkynyl-bridged trinuclear magnesium compound

1. Introduction

Heteroleptic magnesium amides R_2NMgX (R = alkyl, aryl; X = halogen, organyl, amide and alkoxide) is becoming an increasingly active area of research in selective synthesis. Alkylaminomagnesium halides are popularly known as Hauser bases and are valuable tools for the synthetic chemist [1]. For example, Kondo has reported magnesiation of indoles with magnesium amide bases, wherein 1-subsituted indole derivatives are deprotonated with Hauser bases to give magnesindoles, which are then reacted with electrophiles like benzaldehyde or iodine to produce the corresponding substituted indoles in excellent yields [2]. Swiss et al. reported that using the Hauser bases under thermodynamic conditions for antiselectivity in aldol reactions leads to high yields [3]. In addition, Henderson and co-worker described the first example of β-hydride transfer to ketone using an alkyl(amino)magnesium [4]. The high selectivity for these stable products were made possible by reduced steric interactions in transition state. Clearly, a detailed understanding of the solid state structures of heteroleptic magnesium amides would prove useful.

Herein, we report on the synthesis and structural characterization of several heteroleptic magnesium amide compounds in order to extend the investigation of organomagnesium compounds and make a comparison of reactivities between Mg–N(amide) and Mg–X. Moreover, crystallography can provide information on whether it is steric effects or Lewis basicity that acts as

* Corresponding author. Fax: +886-7-5919049.
E-mail address: ccccc@nuk.edu.tw (C.-C. Chang).

0022-328X/02/$ - see front matter
PII: S0022-328X(01)01468-1

a major influence on bridging strength in associated dimeric magnesium structures such as $[R_2NMgX(Sol)]_2$.

2. Results and discussion

2.1. Synthesis

The alkylmagnesium amide $[RMgNPh_2(THF)_2]$ [R = Et **1** or ^{i}Pr **2**] was synthesized by a routine alkane elimination in refluxing at a 1:1 molar ratio of MgR_2 and $HNPh_2$ in THF (Scheme 1). A strong donor solvent HMPA was then added to re-dissolved crystalline **1** in THF leading to isolation of the magnesium bisamide $[Mg(NPh_2)_2(HMPA)_2]$ (**3**). This result showed that an HMPA-induced disproportionation reaction [5] occurred easily (Scheme 2). Compounds of dimeric alkynylmagnesium amide $[(RC{\equiv}C)Mg(\mu\text{-}N^iPr_2)(THF)]_2$ [R=Ph **4** or R=SiMe$_3$ **5**] were prepared using a 1:1 molar ratio of $Mg(N^iPr_2)_2$ and HC≡CR in THF (Scheme 3). The reaction of EtMgBr with $HNEt_2$ or $HN(SiMe_3)_2$ (1:1 molar ratio) in Et_2O or HMPA/THF solution produced different bridged-ligand Hauser bases: $[BrMg(\mu\text{-}NEt_2)(HMPA)]_2$ (**6**) and $[(Me_3Si)_2NMg(\mu\text{-}Br)(OEt_2)]_2$ (**7**), respectively, (Scheme 4). However, the reaction of $MgEt_2$ with $HN(SiMe_3)_2$ produced $[(Me_3Si)_2NMg(\mu\text{-}OEt)(THF)]_2$ (**8**), which involved the intermediate, EtMgOEt (Scheme 5).

Contrary to our expectations, reaction of $Mg(N^iPr_2)_2$ with one molar equivalent of HC≡C^{t}Bu in THF solution did not produce the compound $[(^tBuC{\equiv}C)Mg(\mu\text{-}N^iPr_2)(THF)]_2$, which would have followed following the precedent set by **4** and **5**. Instead two kinds of magnesium acetylide compounds were obtained. One colorless crystal $[(^tBuC{\equiv}C)(THF)Mg(\mu\text{-}C{\equiv}C^tBu)(\mu\text{-}N^iPr_2)Mg(\mu\text{-}C{\equiv}C^tBu)(\mu\text{-}N^iPr_2)Mg(THF)(C{\equiv}C^tBu)]$ (**9**) was isolated from the mixture in refrigerator at 0 °C. Another product $[(^tBuC{\equiv}C)Mg(\mu\text{-}C{\equiv}C^tBu)(THF)]_2$ (**10**) [6] was characterized on the basis of ^{1}H-NMR spectral data (Scheme 6).

2.2. Spectroscopic studies

Compounds **1**–**9** have been characterized with NMR spectroscopy in d_6-benzene solution. In the ^{1}H-NMR, there is one set of quartet and triplet at 0.51, 1.82 ppm for **1** and the other set of septet and doublet at 0.26, 1.81 ppm for **2**, both were assigned as the ethyl and isopropyl groups attached to the magnesium atom. The aromatic protons of **1** and **2** were observed in the region 6.76–7.27 ppm. The spectra of **3** contained two sets of aromatic resonance at 6.71, 6.38 ppm (*p*-H), 7.15, 7.20 ppm (*m*-H), 7.48, 7.50 ppm (*o*-H) in the ^{1}H-NMR and at 115.73, 118.39 ppm (*p*-C), 120.75, 122.13 ppm (*m*-C), 129.45, 129.77 ppm (*o*-C), 144.84, 158.54 ppm (*ipso*-C) in the ^{13}C-NMR. Two sets of methyl resonances for the solvating HMPA groups were also observed at 2.11, 2.38 ppm in the ^{1}H-NMR and 36.50, 37.12 ppm in the ^{13}C-NMR and 24.37, 24.57 ppm in ^{31}P-NMR spectrum. Such appearance is consis-

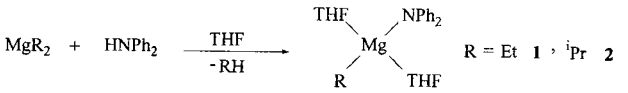

Scheme 1.

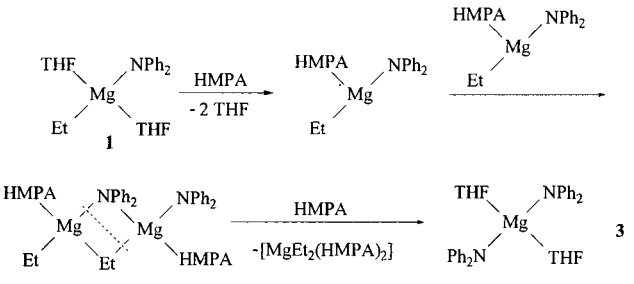

Scheme 2.

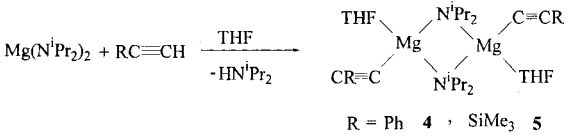

Scheme 3.

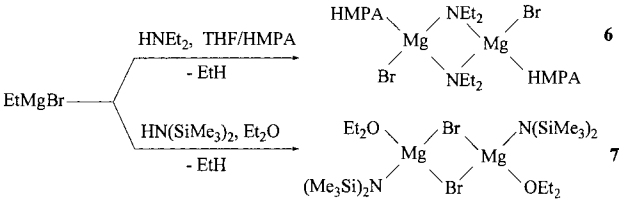

Scheme 4.

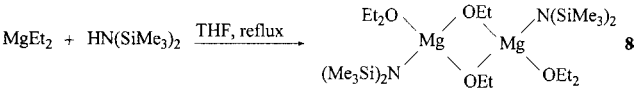

Scheme 5.

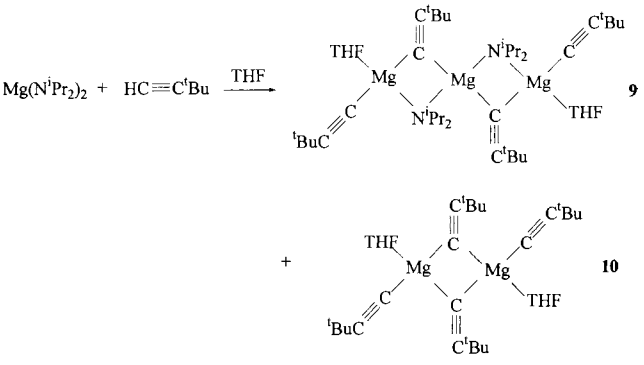

Scheme 6.

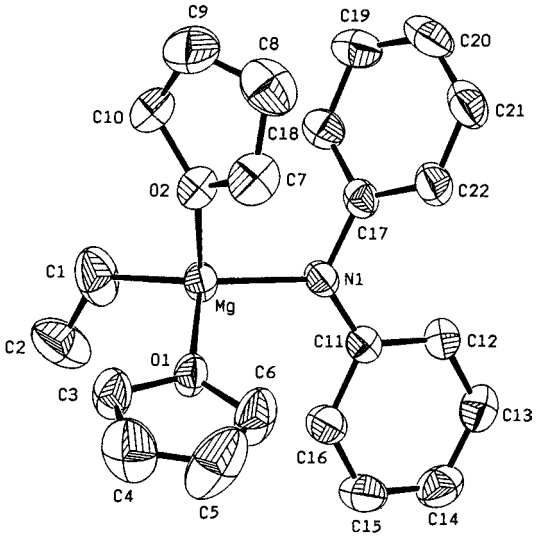

Fig. 1. An ORTEP view of the molecule $[EtMgNPh_2(THF)_2]$ (**1**) using 50% probability ellipsoids. Hydrogen atoms have been omitted for clarity.

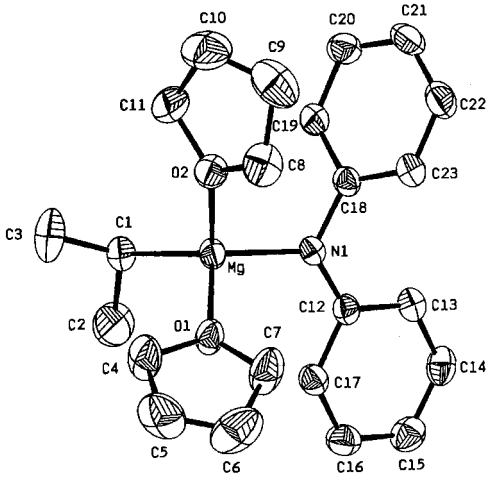

Fig. 2. An ORTEP view of the molecule $[^iPrMgNPh_2(THF)_2]$ (**2**) using 50% probability ellipsoids. Hydrogen atoms have been omitted for clarity.

tent with the asymmetrical structure observed in solid state. In the ^{1}H-NMR, one set of aromatic resonances of C≡CPh group in the region of 6.98–7.86 ppm for **4** and one singlet of $C{\equiv}CSiMe_3$ group at 0.37 ppm for **5** were observed. In the case of **6** two sets of methylene protons at 3.39 and 3.48 ppm were observed for the bridging $N(CH_2CH_3)_2$ groups. Different environments could possibly result from an agostic interaction between magnesium atom and the CH_2 of diethylamido group or from the equilibrium between dimer and monomer in d_6-benzene solution. Furthermore, only one set of doublets was observed at 2.32 ppm for the metal bound HMPA group (away from free HMPA at 2.42 ppm) in compound **6**. For oxidative product **8**, one set of triplets at 1.23 ppm and a quartet at 3.83 ppm were identified as the bridging-ethoxy group.

A 1:2 molar ratio mixture of products **9** and **10** was predicted from the ^{1}H-NMR spectra. Two signals at 0.95 ppm (4H) and 2.79 ppm (24H) were assigned as the isopropyl protons of **9**. One broad peak at 1.43 ppm (108H) was observed. In comparison with one singlet at 1.32 ppm for **10** suggesting the existence of *tert*-butyl protons mixed **9** (36H) and **10** (72H) (ratio 33:67%). Compound **9** was characterized by X-ray crystallography to determine the composition of mixture.

In all IR spectra of compounds **1**–**9**, the metal-ligand bands were observed between 446 and 578 cm^{-1}, which are characteristic of Mg–N, Mg–O and Mg–C stretching vibrations.

2.3. Molecular structures

2.3.1. Monomeric magnesium amide *1*–*3*

The ORTEP views for compounds **1** and **2** are shown in Figs. 1 and 2 and the selected bond and bond angles are listed in Table 1. Both isostructural compounds exhibit a four-coordinate magnesium center, which is bound to one diphenylamido group, one ethyl (or isopropyl) group, and solvated by two molecules of THF to give a distorted tetrahedral arrangement. The geometry is distorted with the smallest bond angles (THF)O–Mg–O(THF) of 93.5(1)° in **1** and 93.31(9)° in **2** and the largest bond angles C–Mg–N of 123.8(2)° in **1** and 122.1(1)° in **2**. Only two crystal structures of alkylmagnesium amides, $[(C_{28}H_{40}N)MgEt(THF)_2]$ [7] and $[(C_{23}H_{28}N_3)MgMe(THF)_2]$ [8], being monomeric because of the steric bulk of its fused heterocyclic ring system, have been reported. The C–Mg–N angles of **1** and **2**, smaller than those observed in the aforementioned compounds (125.2 and 129.30°), might be due to the more bulky nature of the heterocyclic ring ligands. Compound **3** is an asymmetrical bis(amido)magnesium monomer (Fig. 3). The magnesium centre is bound to two diphenylamido groups and solvated by two molecules of HMPA to give a distorted tetrahedron. The bond angle (HMPA)O–Mg–O(HMPA) of 109.11(6)° is larger than those observed in **1** and **2**, due to the basicity or steric repulsion of donor ligands. Small (HMPA)O–Mg–O(HMPA) angles were observed in isostructural bis(amido)magnesium compounds $[Mg(NHMes)_2(HMPA)_2]$ (102.9(4)°) [9] and $[Mg\{N(CH_2Ph)_2\}_2(HMPA)_2]$ (99.7(1)°) [10]. The Mg–N bond lengths of **1**–**3** span a relatively narrow range (2.040(3)–2.056(2) Å), which are consistent with these bond lengths observed in other monomeric bis(amido)magnesium compounds [11]. The Mg–O bond lengths (1.931(1) Å, 1.953(1) Å) for the HMPA ligand in compound **3**, compared with that of (2.037(3)–2.048(2) Å) for the THF in compound **1** and **2**, are in good agreement with the chemical background, where HMPA is stronger donor base than THF.

Additionally, in compounds **1**, **2** and **3** the sum of bond angles around the nitrogen atom is nearly 360°. The C–N–C angles of 118.7–119.2° show that the donor nitrogen atom has an sp^2 structure. In contrast, the C–N–C angles of the analogous dibenzylamido compounds were found at 110.8° for $[Mg\{N(CH_2Ph)_2\}_2(HMPA)_2]$ [10] and 109.6° $[Mg\{N(CH_2Ph)_2\}_2(TMEDA)]$ [10]. These donor nitrogen atoms are formally sp^3 hybridized and easily attack another magnesium atom to form dimer $[Mg\{N(CH_2Ph)_2\}_2(HMPA)]_2$ (C–N–C angle 109.3°) [10].

2.3.2. Dimeric magnesium amides *4*–*8*

Compounds **4**–**8** are dimeric magnesium compounds containing inversion centers. ORTEP views of compounds **4** and **5** are shown in Figs. 4 and 5. Selected bond distances and angles are listed in Table 1. The magnesium atoms are linked by disopropylamino ligands. Each magnesium atom are additionally coordinated one THF molecule with one terminal acetylide PhC≡C or $Me_3SiC{\equiv}C$ group, forming a distorted tetrahedron. In compounds **4** and **5**, the Mg_2N_2 is a planar ring and the bridging Mg–N distances in the 2.116(4)–2.141(5) Å range are consistent with those observed in previous dimeric magnesium amides (2.097–2.147 Å) [12]. The N–Mg–N and Mg–N–Mg angles of 92.8(1) and 87.2(1)° for **4** are close to N–Mg–N and Mg–N–Mg angles of 93.8(2) and 86.2(5)for **5**. In addition, the respective Mg–C bond lengths of 2.134(5) and 2.135(6)Å and the C≡C bond lengths of 1.195(6) and 1.204(8) Å are indistinguishable within the error limits, indicating no influence by different terminal acetylide

Table 1
Selected bond distances (Å) and bond angles (°) for **1**, **2**, **3**, **4** and **5**

$[EtMgNPh_2(THF)_2]$ (**1**)							
Bond distances							
Mg–O(1)	2.039(3)	Mg–O(2)	2.037(3)	Mg–N(1)	2.040(3)	Mg–C(1)	2.098(5)
N(1)–C(3)	1.416(5)	N(1)–C(9)	1.371(5)				
Bond angles							
O(1)–Mg–O(2)	93.5(1)	O(1)–Mg–N(1)	107.5(1)	O(1)–Mg–C(1)	112.9(2)	O(2)–Mg–N(1)	103.6(1)
O(2)–Mg–C(1)	111.1(2)	N(1)–Mg–C(1)	123.8(2)	Mg–N(1)–C(3)	114.7(2)	Mg–N(1)–C(9)	126.1(2)
C(3)–N(1)–C(9)	119.2(3)						
$[^iPrMgNPh_2(THF)_2]$ (**2**)							
Bond distances							
Mg–O(1)	2.048(2)	Mg–O(2)	2.042(2)	Mg–N(1)	2.037(2)	Mg–C(1)	2.131(3)
N(1)–C(12)	1.377(3)	N(1)–C(18)	1.410(3)				
Bond angles							
O(1)–Mg–O(2)	93.31(9)	O(1)–Mg–N(1)	106.65(9)	O(1)–Mg–C(1)	113.0(1)	O(2)–Mg–N(1)	104.57(9)
O(2)–Mg–C(1)	113.2(1)	N(1)–Mg–C(1)	122.1(1)	Mg–N(1)–C(12)	125.7(2)	Mg–N(1)–C(18)	115.6(2)
C(12)–N(1)–C(18)	118.7(2)						
$[Mg(NPh_2)_2(HMPA)_2]$ (**3**)							
Bond distances							
Mg–O(1)	1.953(1)	Mg–O(2)	1.931(1)	Mg–N(1)	2.055(2)	Mg–N(2)	2.056(2)
P(1)–O(1)	1.494(1)	P(2)–O(2)	1.490(1)				
Bond angles							
O(2)–Mg–O(1)	109.11(6)	O(2)–Mg–N(1)	106.07(6)	O(1)–Mg–N(1)	107.99(6)	O(2)–Mg–N(2)	111.78(6)
O(1)–Mg–N(2)	105.10(6)	N(1)–Mg–N(2)	116.61(6)	C(7)–N(1)–C(1)	119.2(1)	C(7)–N(1)–Mg	123.7(1)
C(1)–N(1)–Mg	116.5(1)	C(13)–N(2)–C(19)	118.7(1)	C(13)–N(2)–Mg	118.0(1)	C(19)–N(2)–Mg	123.4(1)
$[(PhC{\equiv}C)Mg(\mu\text{-}N^iPr_2)(THF)]_2$ (**4**)							
Bond distances							
Mg(1)–O(1)	2.091(3)	Mg(1)–N(1)	2.125(4)	Mg(1)–N(1*)	2.116(4)	Mg(1)–C(1)	2.134(5)
C(1)–C(2)	1.195(6)	C(2)–C(3)	1.451(6)				
Bond angles							
O(1)–Mg(1)–N(1)	114.5(1)	O(1)–Mg(1)–N(1*)	117.0(2)	O(1)–Mg(1)–C(1)	92.0(2)	N(1–)Mg(1)–N(1*)	92.8(1)
N(1)–Mg(1-)C(1)	118.9(2)	N(1*)–Mg(1)–C(1)	123.7(2)	Mg(1)–N(1)–Mg(1*)	87.2(1)	Mg–C(1)–C(2)	172.8(5)
$[(Me_3SiC{\equiv}C)Mg(\mu\text{-}N^iPr_2)(THF)]_2$ (**5**)							
Bond distances							
Mg–Mg(a)	2.920(3)	Mg–O	2.098(4)	Mg–N	2.141(5)	Mg–N(a)	2.133(5)
Mg–C(1)	2.135(6)	C(1)–C(2)	1.204(8)				
Bond angles							
O–Mg–N	114.4(2)	O–Mg–N(a)	115.3(2)	O–Mg–C(1)	90.8(2)	N–Mg–N(a)	93.8(2)
N–Mg–C(1)	122.8(2)	N(a)–Mg–C(1)	121.6(2)	Mg–N–Mg(a)	86.2(2)	Mg–C(1)–C(2)	167.8(5)

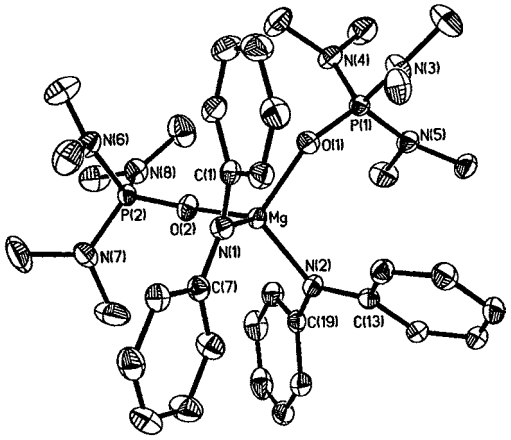

Fig. 3. An ORTEP view of the molecule $[Mg(NPh_2)_2(HMPA)_2]$ (**3**) using 50% probability ellipsoids. Hydrogen atoms have been omitted for clarity.

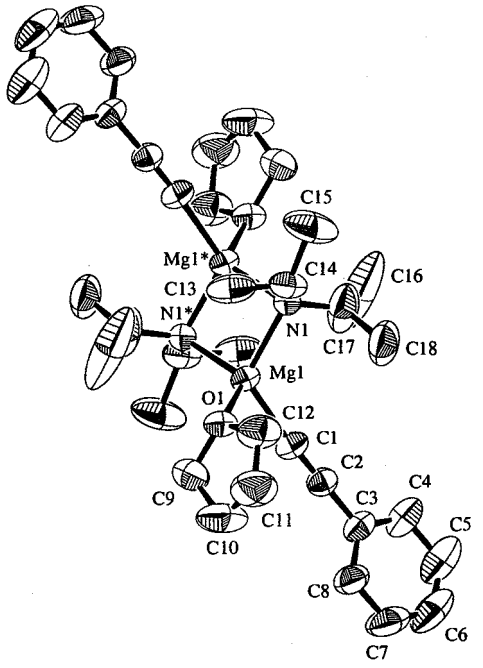

Fig. 4. An ORTEP view of the molecule $[(PhC{\equiv}C)Mg(\mu\text{-}N^iPr_2)(THF)]_2$ (**4**) using 50% probability ellipsoids. Hydrogen atoms have been omitted for clarity.

PhC≡C and $Me_3SiC{\equiv}C$ groups. The terminal Mg–C(ethynyl) bond lengths are slightly shorter than the hexacoordinated magnesium monomer $[Mg(C{\equiv}CPh)_2(tmen)_2]$ (2.176(6), 2.200(6) Å) [13]. However, compound **5** has a sharper Mg–C≡C angle (167.8°) than compound **4** (172.8°), resulting from the steric repulsion of $Me_3SiC{\equiv}C$ ligand.

The ORTEP views of compound **6**, **7** and **8** are shown in Figs. 6–8. Selected bond lengths and bond angles are listed in Table 2. In dimeric compounds **6**, **7** and **8**, the magnesium atoms are linked by bridged ligands diethyl-(amido), bromo and ethoxy, respectively, forming a planar four-membered ring. In compound **6**, Mg_2N_2 core is almost a square planar with Mg–N distances of 2.07(1) Å and internal angles of 91.5(4)° at Mg and 88.5(5)° at N. Each magnesium atom is further coordinated by HMPA (Mg–O = 1.914(1) Å) and a bromine atom (Mg–Br = 2.475(4) Å) with an Br–Mg–O angle of 106.6(3)°. In compound **7**, the Mg_2Br_2 core is also almost a square planar with Mg–Br distances of 2.563(2) and 2.560(2) Å and internal angles of 89.8(1)° at Mg and 90.2(1)° at Br. Each magnesium atom is further coordinated by Et_2O (Mg–O = 2.000(4) Å) and an $N(SiMe_3)_2$ group (Mg–N = 1.962(4) Å) with an O–Mg–N angle of 111.2(2)°. In comparison, the Mg_2O_2 square of compound **8** possesses unequal Mg–O distances, 1.966(2) and 1.942(2) Å, and smaller internal angles of 82.9(1)° at Mg and larger angles of 97.2(2)° at O. Each magnesium atom is further coordinated by THF (Mg–O = 2.051(3) Å) and an $N(SiMe_3)_2$ group (Mg–N = 2.006(3) Å) with an O–Mg–N angle of 103.5(1)°. Similar Mg_2O_2 cores for alkoxo-bridged magnesium compounds favor by O_2 insertion in the mixed-metal Al–Mg compound $[Me_2Al(\mu\text{-}N^iPr_2)_2Mg(\mu\text{-}OMe)]_2$ [14] and *N*,*N*′-dialkyl-aminotroponiminato compound $[Mg(\mu\text{-}OMe)\{(\eta^2\text{-}^iPr_2)ATI\}]_2$ (ATI = *N*-isopropyl-2-(isopropylamino)tropon-imine) [15].

Regarding tetracoordinated magnesium compounds, the bridging Mg–N average distances in **6** are smaller than those in **4**, **5**, $[Mg\{N(CH_2Ph)_2\}_2(HMPA)]_2$ (2.137 Å) [10], $[^nBuMg\{\mu\text{-}N(CH_2CH_2NMe_2)(CH_2Ph)\}]_2$ (2.115 Å) [12a] and $[\{(Me_3Si)_2N\}Mg(\mu\text{-}N(H)Ph)(THF)]_2$ (2.12 Å) [12b], even if tricoordinated magnesium compounds for $[Mg\{N(SiMe_3)_2\}_2]_2$ (2.151 Å) [12c], $[Mg\{N(C_6H_{11})_2\}_2]_2$ (2.11 Å) [9] and $[^sBuMg\{N(SiMe_3)_2\}]_2$ (2.118 Å) [12d] of the latter compounds result from their comparatively crowded amido ligands. The terminal Mg–N distances in **7** and **8** are close to the range of those present in both $[(Me_3Si)NMg(\mu\text{-}Cl)(OEt_2)]_2$ **11** (1.970 Å) [16] and $[\{(Me_3Si)_2N\}Mg(\mu\text{-}OC(H)Ph_2)\text{–}(O{=}CPh_2)]_2$ (2.019 Å) [17].

Bickelhaupt et al. (1991) reported that the bridging ability of X in dimeric structures of $[RMg(\mu\text{-}X)L]_2$ can be summarized as follows: alkoxide, amide > halogen > alkyl, aryl group [18]. The dimeric structure of Hauser base **11** is inconsistent with this sequence. It is important to know which ligand will bridge in the Hauser base R_2NMgX (X = halide). With a more bulky bromine in place of chloride, we also obtained bromo-bridged compound **7**. Compound **11** showed the isostructural features only very little difference from compound **7** in the length of the Mg-halogen bonds ($Mg–Cl_{av.}$ = 2.403 Å). A less bulky NEt_2 ligand replaced $N(SiMe_3)_2$ ligand to change bridging NEt_2 ligand in compound **6**, indicating that increasing the steric bulk of the amide group has the effect of significantly decreasing its bridging ability. A theoretical MO study of heteroleptic pseudo-tetrahedral magnesium compounds predicts that amide is a preferred bridge to

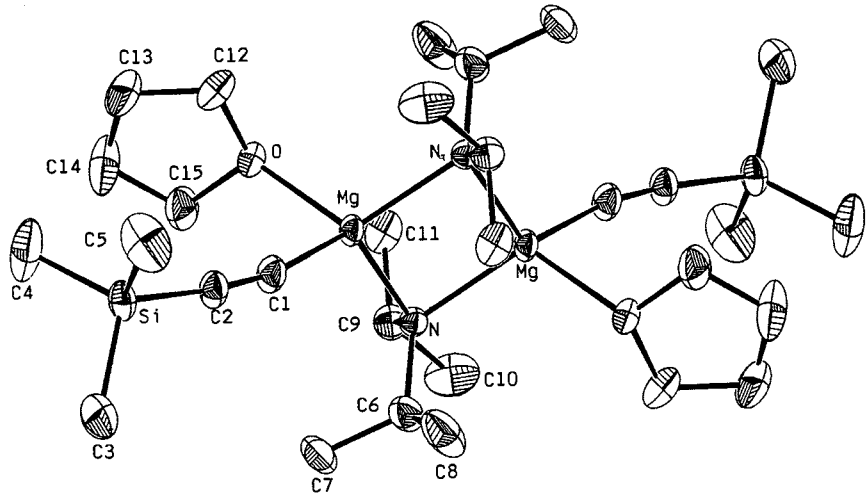

Fig. 5. An ORTEP view of the molecule $[(Me_3SiC{\equiv}C)Mg(\mu\text{-}N^iPr_2)(THF)]_2$ (**5**) using 50% probability ellipsoids. Hydrogen atoms have been omitted for clarity.

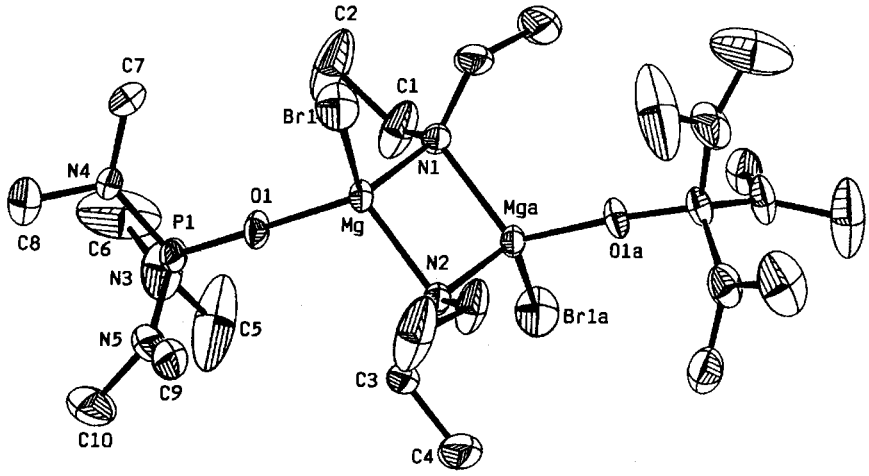

Fig. 6. An ORTEP view of the molecule $[BrMg(\mu\text{-}NEt_2)(HMPA)]_2$ (**6**) using 50% probability ellipsoids. Hydrogen atoms have been omitted for clarity.

halide [17]. This prediction is consistent with the calculated preference for amido bridges and the X-ray data for compound **6** found in our study.

2.3.3. Trimeric magnesium amide *9*

An ORTEP view of compound **9** is shown in Fig. 9. A list of selected bond lengths and angles is provided in Table 2. This compound contains three magnesium atoms with distorted tetrahedron geometries, each linked with pairs of bridging N^iPr_2 and $C{\equiv}C^tBu$ ligands. Magnesium compounds exhibiting both electron-rich and electron-deficient bridging ligand are rarely observed. Different bridging ligands also give two heterocyclic four-membered rings Mg_2CN, not coplanar ring. The outer magnesium atoms Mg(1) and Mg(2) are additionally coordinated by a terminal ligand $C{\equiv}C^tBu$

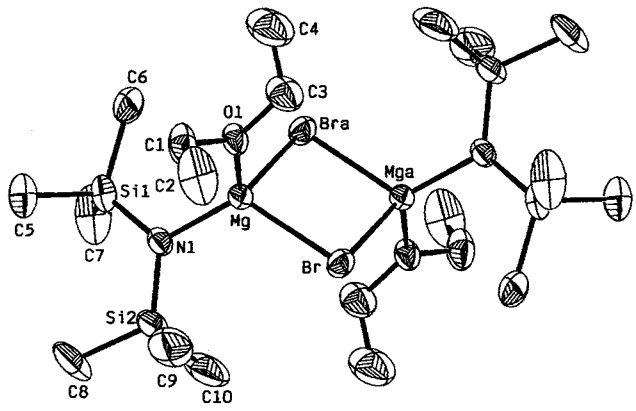

Fig. 7. An ORTEP view of the molecule $[(Me_3Si)_2NMg(\mu\text{-}Br)(OEt_2)]_2$ (**7**) using 50% probability ellipsoids. Hydrogen atoms have been omitted for clarity.

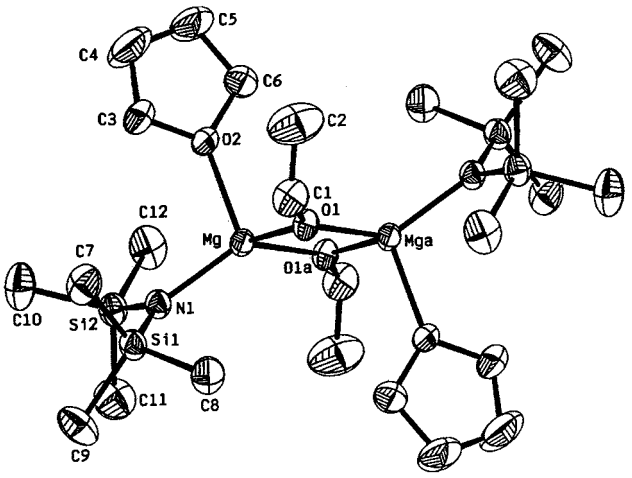

Fig. 8. An ORTEP view of the molecule $[(Me_3Si)_2NMg(\mu\text{-}OEt)(THF)]_2$ (**8**) using 50% probability ellipsoids. Hydrogen atoms have been omitted for clarity.

and a THF molecule. The bridging Mg–C_α(ethynyl) distances ranging from 2.203(2) to 2.225(2) Å are similar to those in $[Me_2Al(\mu\text{-}N^iPr_2)_2Mg(\mu\text{-}^t BuC{\equiv}C)]_2$ (2.201(9) and 2.225(8) Å) [19]. These distances are somewhat longer than the terminal Mg–C_α(ethynyl) distances of 2.100(2) and 2.092(2) Å in **9** and 2.175(4) Å in $[Mg(^t BuC{\equiv}C)_2(tmen)_2]$ [20]. Moreover, Mg–C_α–Mg and Mg–N–Mg bond angle of 84.83 and 90.30° were found in the Mg(1)C(1)Mg(2)N(1) ring [cf. the corresponding angles of 85.02 and 88.89° were found in Mg(2)C(13)Mg(3)N(2) ring]. The difference between Mg–C_α–Mg and Mg–N–Mg resulted from the weak repulsion of a two-electron-three-center bond Mg–C_α relative to a four-electron-three-center bond Mg–N.

The μ-^{t}BuC≡C ligands tilt toward Mg(1) and Mg(3). The Mg(1)–C(1)≡C(2) angle of 92.4(2)° is much smaller than Mg(2)–C(1)≡C(2) angle of 173.2(2)°. Similarly, the Mg(3)–C(13)≡C(14) angle of 96.4(2)° is much smaller than the Mg(2)–C(13)≡C(14) angle of 163.6(2)°. Hence, an unusual Mg–C_α distance differentiation was observed: Shorter σ-Mg(2)–C(1) (2.206 Å), σ-Mg(2)–C(13) (2.203 Å) and longer π-Mg(1)–C(1) (2.255 Å), π-Mg(3)–C(13) (2.240 Å). Moreover, Mg(1)–C(2) (2.609 Å) and Mg(3)–C(14) (2.668 Å) are shorter than the sum of their van der waals radii (ca. 3.4 Å), revealing that a strong π-interaction between μ-^{t}BuC≡C ligands and magnesium atoms exists. A similar structure with bridging type 3e donors, involving in σ- and π-type interaction was observed for $[(MeC{\equiv}C)Be(\mu\text{-}C{\equiv}CMe)(NMe_3)]_2$ [21].

The structure of **9** reveals a rare example of trinuclear magnesium amide. Its bridging Mg–N distances, in the range of 2.117(2)–2.159(2) Å, are close to those observed for the bridging Mg–N bonds in **4** and **5**. Other solvent-free trinuclear species $[Mg_3\{\mu\text{-}N(H)(Dipp)\}_4\{N(SiMe_3)_2\}_2]$, (Dipp = 2,6-^{i}Pr$_2C_6H_3$) [9], reported by Power, to contain an 2:1 ratio of its two distinct amides ligands and the bridging Mg–N distances, lie in the range of 2.090(6)–2.128(6) Å.

3. Experimental

All experiments were carried out in an N_2 flushed glovebag, in a dry box or in vacuum using standard Schlenk techniques. The magnesium metals, $HNEt_2$, HN^iPr_2, $HNPh_2$ and $HN(SiMe_3)_2$ were purchased from Aldrich and use as received. EtMgBr, $MgEt_2$, Mg^iPr_2, $Mg(N^iPr_2)_2$ [22] were prepared according to previous reports. All solvents were distilled and degassed prior to use. All ^{1}H, ^{13}C, and ^{31}P spectra were measured on a Varian-300 spectrometer. Chemical shifts are made with reference to either TMS(^{1}H) or C_6D_6(^{1}H, δ 7.15; ^{13}C{^{1}H}, 128.00). ^{31}P-NMR spectra are made with reference external 85% H_3PO_4. Mass spectra data were obtained on a VG-7025 GC–MS–MS spectrometer. IR spectra data were obtained on a FTIR spectrometer. Elemental analyses (C, H, and N) were performed at the Analytsche Laboratorien of H. Malissa and G. Reuter GmbH, Germany. Deviation in the results from calculated values are attributed to the extremely air-sensitive and hygroscopic nature of these compounds.

3.1. $[RMgNPh_2(THF)_2]$ [R = Et **1**, ^{i}Pr **2**]

$HNPh_2$ (18.7 mmol) in THF (20 ml) was added dropwise to a refluxing THF (100 ml) solution of MgR_2 (18.7 mmol). After 3 h, the mixture was centrifuged and a partial volume of solvent was removed in vacuum. The solution was then cooled in refrigerator for 1 day, and large block crystals formed.

3.2. $[EtMgNPh_2(THF)_2]$ (**1**)

Melting point (decomposition) (m.p. (dec.)) > 104 °C, yield = 78%, ^{1}H-NMR (C_6D_6): δ 0.51 (q, 2H, CH_2CH_3), 1.11 (m, 8H, 3, 4-thf–H), 1.82 (t, 3H, CH_2CH_3), 3.34 (m, 8H, 2, 5-thf–H), 6.76–7.19 (m, 10H, C_6H_5). ^{13}C-NMR (C_6D_6): δ 1.39 (CH_2CH_3), 14.32 (CH_2CH_3), 25.59 (3, 4-thf–C), 69.39 (2, 5-thf–C), 117.70 (*p*-C), 121.68 (*m*-C), 130.06 (*o*-C), 157.02 (*ipso*-C). Mass spectrum (EI: 70 eV) ten most intense *m*/*e*: 169, 168, 42, 167, 51, 84, 71, 72, 77, 43. IR (KBr, cm^{-1}): 3409 m, 3382 s, 3039 w, 2964 w, 1594 s, 1520 s, 1492 s, 1456 m, 1415 m, 1318 s, 1260 m, 1173 m, 1084 m, 1021 m, 877 m, 800 m, 749 s, 701 m, 689 s, 642 m, 569 m, 503 m. Anal. Calc. for $C_{22}H_{31}MgNO_2$: C, 72.24; H, 8.54; N, 3.83. Found: C, 72.66; H, 8.76; N, 3.99%.

3.3. $[^iPrMgNPh_2(THF)_2]$ (**2**)

M.p. = 133–135 °C, yield = 60%, ^{1}H-NMR (C_6D_6): δ 0.26 [sep, 1H, $CH(CH_3)_2$], 1.17 (m, 8H, 3, 4-thf–H),

1.81 [d, 6H, $CH(CH_3)_2$], 3.38 (m, 8H, 2, 5-thf–H), 6.77–7.27 (m, 10H, C_6H_5). ^{13}C-NMR (C_6D_6): δ 9.63 [$CH(CH_3)_2$], 25.48 (3, 4-thf–C), 26.39 [$CH(CH_3)_2$], 69.53 (2, 5-thf–C), 116.99 (*p*-C), 117.66 (*p*-C), 121.27 (*m*-C), 121.61 (*m*-C), 129.99 (*o*-C), 130.10 (*o*-C), 156.99 (*ipso*-C), 157.45 (*ipso*-C). Mass spectrum (EI: 70 eV) ten most intense *m*/*e*: 169, 168, 42, 167, 51, 84, 71, 72, 77, 43. IR (KBr, cm^{-1}): 3406 m, 3383 s, 3042 w, 2959 m, 2924 m, 2854 m, 1596 s, 1519 s, 1494 s, 1458 m, 1417 m, 1384 m, 1317 m, 1261 w, 1244 w, 1173 m, 1084 m, 1024 m, 876 w, 801 w, 749 s, 701 m, 690 s, 502 m.

3.4. $[Mg(NPh_2)_2(HMPA)_2]$ (3)

The compound **1** 2.7 g (7.4 mmol) was dissolved in the 10 ml HMPA/THF (2:3) solvent. The solution was then allowed to set at room temperature (r.t.) with slow evaporation of solvent until large block crystals formed. M.p. = 164–166 °C, yield = 36%, ^{1}H-NMR (C_6D_6): δ 2.11, 2.38 [d, 36H, $(Me_2N)_3PO$], 6.71, 6.38 (m, 4H, *p*-H), 7.15, 7.20 (m, 8H, *m*-H), 7.48, 7.50 (d, 8H, *o*-H). ^{13}C-NMR (C_6D_6): δ 36.50 $(Me_2N)_3PO$], 37.12 [$(Me_2N)_3PO$], 115.73 (*p*-C), 118.39 (*p*-C), 120.75 (*m*-C), 122.13 (*m*-C), 129.45 (*o*-C), 129.77 (*o*-C), 144.84 (*ipso*-C), 158.54 (*ipso*-C). ^{31}P-NMR (C_6D_6): δ 24.37 [$(Me_2N)_3PO$], 24.57 [$(Me_2N)_3PO$]. Mass spectrum (EI: 70 eV) ten most intense *m*/*e*: 169, 135, 44, 168, 45, 167,179, 180, 92, 42. IR (KBr, cm^{-1}): 3116 m, 2845 m, 2802 m, 1593 s, 1535 m, 1495 s, 1460 s, 1314 s, 1199 s, 1067 m, 983 s, 878 w, 747 s, 695 m, 569 w, 505 m, 481 m. Anal. Calc. for $C_{36}H_{56}MgN_8O_2P_2$: C, 60.13; H, 7.85; N, 15.58. Found: C, 60.12; H, 8.03; N, 15.68%.

Table 2
Selected bond distances (Å) and bond angles (°) for **6**, **7**, **8** and **9**

$[BrMg(\mu\text{-}NEt_2)(HMPA)]_2$ (**6**)							
Bond distances							
Mg–Mg(a)	2.892(7)	Mg–Br(1)	2.475(4)	Mg–O(1)	1.914(7)	Mg–N(1)	2.07(1)
Mg–N(2)	2.07(1)	P(1)–O(1)	1.478(7)				
Bond angles							
Br(1)–Mg–O(1)	106.6(3)	Br(1)–Mg–N(1)	112.7(2)	Br(1)–Mg–N(2)	119.1(2)	O(1)–Mg–N(1)	115.8(3)
O(1)–Mg–N(2)	111.1(3)	N(1)–Mg–N(2)	91.5(4)	Mg–O(1)–P(1)	175.1(5)	Mg–N(1)–Mg(a)	88.5(5)
Mg–N(2)–Mg(a)	88.6(5)						
$[(Me_3Si)_2NMg(\mu\text{-}Br)(OEt_2)]_2$ (**7**)							
Bond distances							
Mg–Br	2.563(2)	Mg–Br(a)	2.560(2)	Mg–O(1)	2.000(4)	Mg–N(1)	1.962(4)
Br–Mg–Br(a)	89.81(5)	Br–Mg–O(1)	100.6(1)	Br–Mg–N(1)	121.2(1)	Br(a)–Mg–O(1)	107.3(1)
Bond angles							
Br(a)–Mg–N(1)	122.0(1)	O(1)–Mg–N(1)	112.2(2)	Mg–Br–Mg(a)	90.19(5)		
$[(Me_3Si)_2NMg(\mu\text{-}OEt)(THF)]_2$ (**8**)							
Bond distances							
Mg–Mg(a)	2.930(2)	Mg–O(1)	1.966(2)	Mg–O(1a)	1.942(2)	Mg–O(2)	2.051(3)
Mg–N(1)	2.006(3)						
Bond angles							
O(1)–Mg–O(1a)	82.9(1)	O(1)–Mg–O(2)	100.2(1)	O(1)–Mg–N(1)	129.2(1)	O(1a)–Mg–O(2)	109.9(1)
O(1a)–Mg–N(1)	127.9(1)	O(2)–Mg–N(1)	103.5(1)	Mg–O(1)–Mg(a)	97.2(1)		
$[(^tBuC{\equiv}C)(THF)Mg(\mu\text{-}C{\equiv}C^tBu)(\mu\text{-}N^iPr_2)Mg(\mu\text{-}C{\equiv}C^tBu)(\mu\text{-}N^iPr_2)Mg(THF)(C{\equiv}C^tBu)]$ (**9**)							
Bond distances							
Mg(1)–O(1)	2.057(2)	Mg(1)–C(7)	2.100(2)	Mg(1)–N(1)	2.117(2)	Mg(1)–C(1)	2.255(2)
Mg(1)–C(2)	2.609(3)	Mg(1)–Mg(2)	3.010(1)	Mg(2)–N(1)	2.138(2)	Mg(2)–N(2)	2.159(2)
Mg(2)–C(13)	2.203(2)	Mg(2)–C(1)	2.206(3)	Mg(2)–Mg(3)	3.003(1)	Mg(3)–O(2)	2.060(2)
Mg(3)–C(19)	2.092(3)	Mg(3)–N(2)	2.129(2)	Mg(3)–C(13)	2.240(2)	Mg(3)–C(14)	2.668(2)
C(1)–C(2)	1.222(3)	C(13)–C(14)	1.220(3)				
Bond angles							
O(1)–Mg(1)–C(7)	100.99(9)	O(1)–Mg(1)–N(1)	110.77(9)	C(7)–Mg(1)–N(1)	125.39(10)	O(1)–Mg(1)–C(1)	98.63(8)
C(7)–Mg(1)–C(1)	128.0(1)	N(1)–Mg(1)–C(1)	90.30(8)	N(1)–Mg(2)–N(2)	137.42(9)	N(1)–Mg(2)–C(13)	111.51(9)
N(2)–Mg(2)–C(13)	90.99(8)	N(1)–Mg(2)–C(1)	91.07(8)	N(2)–Mg(2)–C(1)	116.37(8)	C(13)–Mg(2)–C(1)	108.38(9)
O(2)–Mg(3)–C(19)	101.8(1)	O(2)–Mg(3)–N(2)	120.86(8)	C(19)–Mg(3)–N(2)	119.6(1)	O(2)–Mg(3)–C(13)	95.31(8)
C(19)–Mg(3)–C(13)	128.0(1)	N(2)–Mg(3)–C(13)	90.77(8)	Mg(1)–N(1)– Mg(2)	90.01(9)	Mg(3)–N(2)– Mg(2)	88.89(7)
C(2)–C(1)–Mg(2)	173.2(2)	C(2)–C(1)–Mg(1)	92.4(2)	Mg(2)–C(1)–Mg(1)	84.83(9)	C(14)–C(13)–Mg(2)	163.6(2)
C(14)–C(13)–Mg(3)	96.4(2)	Mg(2)–C(13)–Mg(3)	85.02(8)				

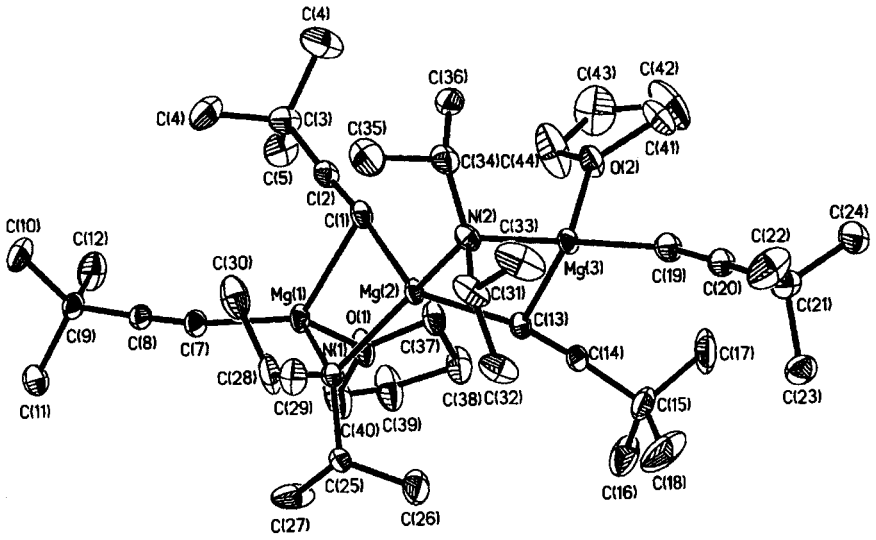

Fig. 9. An ORTEP view of the molecule [('BuC≡C)(THF)Mg(μ-C≡C'Bu)(μ-N^{i}Pr$_2$)Mg(μ-C≡C'Bu)(μ-N^{i}Pr$_2$)Mg(THF)(C≡C'Bu)] (**9**) using 30% probability ellipsoids. Hydrogen atoms have been omitted for clarity.

3.5. [(RC≡C)Mg(μ-N^{i}Pr$_2$)(THF)]$_2$ [R = Ph **4**, SiMe$_3$ **5**]

RC≡CH (R = Ph or SiMe$_3$) (12 mmol) in THF (10 ml) was added dropwise to a THF (80 ml) solution of Mg(N^{i}Pr$_2$)$_2$ (12 mmol). The reaction mixture stirred for 18 h at r.t.. The light yellow color of the solution turned brown. After centrifuging, some solvent was removed in vacuum, then hexane (10 ml) was added. The solution was cooled in refrigerator for one day, and colorless crystals formed.

3.6. [(PhC≡C)Mg(μ-N^{i}Pr$_2$)(THF)]$_2$ (**4**)

^{1}H-NMR (C$_6$D$_6$): δ 0.97 [d, 24H, CH(CH$_3$)$_2$], 1.35 (m, 8H, 3, 4-thf–H), 2.78 [sep, 4H, CH(CH$_3$)$_2$], 3.72 (m, 8H, 2, 5-thf–H), 6.98 (m, 2H, *p*-H), 7.16 (m, 4H, *m*-H), 7.86 (m, 4H, *o*-H). ^{13}C-NMR (C$_6$D$_6$): δ 23.6 [CH(CH$_3$)$_2$], 25.5 (3, 4-thf–C), 45.2 [CH(CH$_3$)$_2$], 68.2 (2, 5-thf–C), 121.4 (*p*-C), 126.3 (*m*-C), 132.2 (*o*-C). Mass spectrum (EI: 70 eV) ten most intense *m*/*e*: 102, 60, 43, 69, 76, 117, 86, 81, 149, 58. IR (Nujol, cm^{-1}): 3074 m, 2926 m, 2869 m, 2075 m, 1963 m, 1089 w, 1788 w, 1680 m, 751 m, 692 m.

3.7. [(Me$_3$SiC≡C)Mg(μ-N^{i}Pr$_2$)(THF)]$_2$ (**5**)

^{1}H-NMR (C$_6$D$_6$): δ 0.37 (s, 18H, Me$_3$Si), 0.94 [d, 24H, CH(CH$_3$)$_2$], 1.49 (m, 8H, 3, 4-thf–H), 2.78 [sep, 4H, CH(CH$_3$)$_2$], 3.76 (m, 8H, 2, 5-thf–H). ^{13}C-NMR (C$_6$D$_6$): δ 0.9 [Me$_3$Si], 23.7 [CH(CH$_3$)$_2$], 25.7 (3, 4-thf–C), 45.3 [CH(CH$_3$)$_2$], 68.3 (2, 5-thf–C). Mass spectrum (EI: 70 eV) ten most intense *m*/*e*: 86, 44, 73, 58, 155, 101, 125, 53, 197, 221. IR (Nujol, cm^{-1}): 2961 m, 2925 m, 2871 m, 2028 s, 1461 s, 1381 s, 1247 s, 1155 s, 1021 s, 981 m.

3.8. [BrMg(μ-NEt$_2$)(HMPA)]$_2$ (**6**)

HNEt$_2$ (1.42 g, 19.4 mmol) and HMPA (3.49 g, 19.4 mmol) in THF (20 ml) was added dropwise to a THF (100 ml) solution of EtMgBr (19.5 mmol). The reaction mixture was stirred for 6 h at r.t.. A purification and crystallization procedure similar to that for the compound **1** was used. M.p.$_{dec}$ > 63 °C, yield = 51%, ^{1}H-NMR (C$_6$D$_6$): δ 1.59 [t, 12H, N(CH$_2$CH$_3$)$_2$], 2.32 [d, 36H, (Me$_2$N)$_3$PO], 3.39 [m, 4H, N(CH$_2$CH$_3$)$_2$], 3.48 [m, 4H, N(CH$_2$CH$_3$)$_2$]. ^{13}C-NMR (C$_6$D$_6$): δ 16.23 [N(CH$_2$-CH$_3$)$_2$], 37.12 (Me$_2$N)$_3$PO], 43.17 [N(CH$_2$CH$_3$)$_2$]. ^{31}P-NMR (C$_6$D$_6$): δ 25.59 [(Me$_2$N)$_3$PO]. Mass spectrum (FAB+) ten most intense *m*/*e*: 135, 180, 642, 535, 74, 136, 370, 463, 640, 281. IR (KBr, cm^{-1}): 3340 s, 2939 sh, 2857 s, 2809 s, 2686 m, 2460 m, 2358 m, 1952 m, 1753 m, 1638 m, 1488 s, 1462 s, 1386 s, 1307 s, 1195 s, 1158 s, 1067 s, 999 s, 795 m, 761 s, 603 s, 532 s, 483 s.

3.9. [(Me$_3$Si)$_2$NMg(μ-Br)(OEt$_2$)]$_2$ (**7**)

A similar procedure was used, except for the use of HN(SiMe$_3$)$_2$ as HNEt$_2$ in Et$_2$O solution. M.p.$_{dec}$ > 120 °C, yield = 39%, ^{1}H-NMR (C$_6$D$_6$): δ 0.42 (s, 36H, Me$_3$Si), 0.95 (t, 12H, CH$_3$CH$_2$OCH$_2$CH$_3$), 3.53 (q, 8H, CH$_3$CH$_2$OCH$_2$CH$_3$). ^{13}C-NMR (C$_6$D$_6$): δ 6.82 (Me$_3$Si), 14.46 (*C*H$_3$CH$_2$OCH$_2$*C*H$_3$), 66.05 (CH$_3$CH$_2$OCH$_2$-CH$_3$). Mass spectrum (FAB+) ten most intense *m*/*e*: 324, 411, 329, 409, 460, 442, 440, 330, 360, 391. IR (KBr, cm^{-1}): 3416 s, 2961 m, 1631 sh, 1405 m, 1386 m, 1262 w, 1101 w, 1030 w, 805 w, 603 s, 446 m. Anal. Calc. for C$_{20}$H$_{56}$Mg$_2$N$_8$O$_2$Si$_4$Br$_2$: C, 35.42; H, 8.33; N, 4.15. Found: C, 34.44; H, 8.14; N, 4.26%.

3.10. $[(Me_3Si)_2NMg(\mu\text{-}OEt)(THF)]_2$ (8)

The synthetic procedure was similar to those used for compounds **1** and **2**, using $HN(SiMe_3)_2$ (28 mmol). M.p. = 132–134 °C, yield = 27%, ^{1}H-NMR (C_6D_6): δ 0.35 (s, 36H, Me_3Si), 1.23 (t, 6H, OCH_2CH_3), 1.31 (m, 8H, 3, 4-thf–H), 3.69 (m, 8H, 2, 5-thf–H), 3.83 (q, 4H, OCH_2CH_3). ^{13}C-NMR (C_6D_6): δ 6.67 (Me_3Si), 22.30 (OCH_2CH_3), 25.49 (3, 4-thf–C), 58.61 (OCH_2CH_3), 69.74 (2, 5-thf–C). Mass spectrum (EI: 70 eV) ten most intense m/e: 146, 130, 147, 66, 73, 100, 45, 148, 43, 161. IR (KBr, cm^{-1}): 3428 m, 2955 w, 2862 w, 1631 w, 1467 m, 1381 m, 1256 w, 1128 w, 1064 w, 983 w, 836 w, 746 w, 513 s. Anal. Calc. for $C_{24}H_{62}Mg_2N_8O_4Si_4$: C, 47.70; H, 10.35. Found: C, 47.88; H, 10.23%.

3.11. Reaction of $Mg(N^iPr_2)_2$ with $HC{\equiv}C^tBu$

A procedure similar to that for compounds **4** and **5** was used, except for using ^{t}BuC≡CH (33 mmol) and $Mg(N^iPr_2)_2$ (33 mmol). ^{1}H-NMR spectroscopy showed that these crystals were a mixture of two compounds, probably $[(^t\text{BuC}{\equiv}\text{C})(\text{THF})\text{Mg}(\mu\text{-}^t\text{BuC}{\equiv}\text{C})(\mu\text{-N}^i\text{Pr}_2)\text{Mg}(\mu\text{-}^t\text{BuC}{\equiv}\text{C})(\mu\text{-N}^i\text{Pr}_2)\text{Mg}(\text{THF})(\text{C}{\equiv}\text{C}^t\text{Bu})]$ **9** and $[(^t\text{BuC}{\equiv}\text{C})\text{Mg}(\mu\text{-}^t\text{BuC}{\equiv}\text{C})(\text{THF})]_2$ (**10**). ^{1}H-NMR (C_6D_6): δ 0.95 [d, 24H, $CH(CH_3)_2$], 1.43 [br, 108H, $C(CH_3)_3$], 1.64 (m, 24H, 3, 4-thf–H), 2.79 [m, 4H, $CH(CH_3)_2$], 3.71 (m, 24H, 2, 5-thf–H).

4. Structure determination

Crystals used for X-ray measurements were sealed in glass capillaries at room temperature and cooled to 150 K (**3** and **9**) in a N_2 cold stream. Preliminary examinations and intensity data collections were carried out with an Enraf-Nonius CAD4 automatic diffractometer (for **1**, **2** and **5**–**8**), Bruker SMART CCD automatic diffractometer (for **3** and **9**) or a Rigaku AFC7S diffractometer (for **4**) using graphite-monochromatized Mo–K_α radiation ($\lambda = 0.71069$ Å). Intensity data were collected using the θ–2θ scan mode and corrected for absorption and decay. The structures were solved by direct method and refined with full-matrix least squares on F (for **1**, **2** and **4**–**8**) or on F^2 (for **3** and **9**). In the final cycles all non-hydrogen atoms were refined anisotropically and all hydrogen atoms were fixed at idealized positions. All calculations were carried out with a α 3500 computer using NRC VAX program [23] (for **1**, **2** and **5**–**8**), a PC computer using SHELXTL program (for **3** and **9**) or a SGIR4000 computer using the TEXSAN program [22] (for **4**). In compound **1**, ethyl group is disordered. Site occupancy of 50% was assigned for each of disorder carbon atoms (C2 and C2′). In compound **9**, one terminal butyl group of C≡C′Bu ligand is disordered. The pairs of carbon atoms C(10), C(10′); C(11), C(11′); C(12), C(12′) have the ratio of 75/25% occupancies. Also, two isopropyl groups are

Table 3
Crystal and intensity collection data for compounds **1**, **2**, **3**, **4** and **5**

	1	**2**	**3**	**4**	**5**
Empirical Formula	$C_{22}H_{31}MgNO_2$	$C_{23}H_{33}MgNO_2$	$C_{36}H_{56}MgN_8O_2P_2$	$C_{36}H_{54}Mg_2N_2O_2$	$C_{30}H_{62}Mg_2N_2O_2Si_2$
Formula weight	366.30	379.82	719.14	595.44	587.61
Crystal system	Monoclinic	Monoclinic	Monoclinic	Monoclinic	Monoclinic
Space group	$P2_1/n$	$P2_1/n$	$P2_1/n$	$P2_1/c$	$P2_1/c$
a (Å)	9.7833(20)	9.9886(14)	12.1181(1)	8.851(2)	14.793(4)
b (Å)	14.9810(21)	15.0909(12)	19.2188(3)	11.048(2)	10.145(3)
c (Å)	14.7258(15)	14.8518(19)	17.4236(2)	19.149(1)	14.635(6)
β (°)	91.020(15)	92.650(12)	95.779(1)	98.92(1)	119.123(3)
V (Å^3)	2157.9 (6)	2236.3(5)	4037.25(9)	1849.7(4)	1918.8(11)
Z	4	4	4	2	2
D_{calc}, (g cm^{-3})	1.127	1.128	1.183	1.069	1.017
Absorption coefficient (cm^{-1})	0.916	0.905	1.64	0.95	2.891
$F(000)$	794	824	1544	3312	649
Crystal size (mm)	$0.70 \times 0.60 \times 0.50$	$0.60 \times 0.60 \times 0.60$	$0.50 \times 0.50 \times 0.40$	$0.33 \times 0.33 \times 0.48$	$0.25 \times 0.70 \times 0.70$
2θRange (°)	18.80–30.00	18.88–33.36	3.16–55.00	15.5–22.8	14.00–24.20
Reflection collected	3794	3917	22 096	3109	2494
Reflection observed [$I > 2\sigma(I)$]	2060	2526	9092	1524 ($I > 3\sigma(I)$)	1458
Transmission factor	0.903, 0.948	0.914, 0.957	0.8370, 0.9623	0.9476, 1.0000	0.910, 1.000
Temperature (K)	295	295	150	297	298
Goodness of fit	1.63	1.58	1.071	2.63	1.36
R_f, R_w	0.052, 0.047	0.047, 0.042	0.0462, 0.1023	0.056, 0.052 [a]	0.063, 0.062
Largest difference peak and hole (e Å^{-3})	0.160, −0.180	0.210, −0.170	0.268, −0.300	0.29, −0.27	0.410, −0.290

$R_f = \Sigma||F_o| - |F_c||/\Sigma|F_o|$; $Rw = [\Sigma w(F_o - F_c)^2/\Sigma wF_o^2]^{1/2}$.
[a] $w = [\sigma^2(F_o)]^{-1} = [\sigma_c^2(F_o) + P^2/4F_o^2]^{-1}$, $P = 0.0090$.

Table 4
Crystal and intensity collection data for compounds **6**, **7**, **8** and **9**

	6	**7**	**8**	**9**
Empirical Formula	$C_{20}H_{56}N_8O_2P_{26}Mg_2Br_2$	$C_{20}H_{56}N_2O_2Si_4Mg_2Br_2$	$C_{24}H_{62}N_2O_4Si_4Mg_2$	$C_{44}H_{80}N_2O_2Mg_3$
Formula weight	711.07	677.43	603.71	742.03
Crystal system	Orthorhombic	Monoclinic	Monoclinic	Triclinic
Space group	*P bcn*	$P2_1/c$	$P2_1/n$	$P\bar{1}$
a (Å)	10.272(3)	10.6194(20)	10.737(3)	12.1898(2)
b (Å)	16.6235(18)	14.006(3)	12.4791(19)	13.2651(2)
c (Å)	21.666(3)	13.508(3)	14.3045(18)	16.1646(2)
α (°)	–	–	–	80.096(1)
β (°)	–	105.479(21)	94.79(3)	77.953(1)
γ (°)	–	–	–	74.469(1)
V (Å^3)	3699.6(13)	1936.2(7)	1909.9(7)	2444.12(6)
Z	4	2	2	2
D_{calc} (g cm^{-3})	1.277	1.162	1.050	1.008
Absorption coefficient (cm^{-1})	23.182	22.419	2.087	0.95
F(000)	1487	712	665	820
Crystal size (mm)	$0.60\times0.60\times0.40$	$0.50\times0.50\times0.40$	$0.60\times0.60\times0.50$	$0.50\times0.40\times0.40$
2θRange (°)	17.64–26.50	16.00–20.28	16.56–26.48	2.60–52.74
Reflection collected	3249	3400	3348	25667
Independent reflections	3249	3400	3348	9683 ($R_{int}=0.0309$)
Observed reflections [$I>2\sigma(I)$]	996	1550	2341	–
Transmission factor	0.313, 0.430	0.327, 0.448	0.820, 0.912	0.7130, 0.9280
Temperature (K)	295	295	295	150
Goodness of fit	2.66	1.67	1.77	1.053
R_f, R_w	0.058, 0.057	0.040, 0.034	0.048, 0.047	0.0649, 0.1575
Largest difference peak and hole (e Å^{-3})	0.710, −0.400	0.250, −0.190	0.390, −0.240	0.504, −0.262

$Rf=\Sigma||F_o|-|F_c||/\Sigma|F_o|$; $Rw=[\Sigma w(F_o-F_c)^2/\Sigma wF_o^2]^{1/2}$.

disordered. All atoms of C(25), C(25′); C(29), C(29′) have the half occupancies. A summary of the data collection and structure solution is given in Tables 3 and 4.

5. Supplementary material

Crystallographic data for the structural analysis have been deposited with the Cambridge Crystallographic Data Centre, CCDC no. 158070–158077 for compound **1**–**3** and **5**–**9** and 158616 for compound **4**. Copies of this information may be obtained free of charge from the Director, CCDC, 12 Union Road, Cambridge CB2 1ZE, UK (Fax: +44-1223-336033; or email: deposit@ccdc.cam.ac.uk or www: http://www.ccdc.cam.ac.uk).

Acknowledgements

We thank the National Science Council, Taiwan, ROC, for financial support.

References

[1] (a) E.C. Ashby, A.B.J. Goel, Inorg. Chem. 17 (1978) 1862;
(b) J.K. Stille, W.J. Scott, J. Am. Chem. Soc. 108 (1986) 3033;
(c) D. Bonafoux, M. Bordeau, C. Brian, P. Cazeau, J. Org. Chem. 61 (1996) 5532;
(d) K. Kobayashi, M. Kawakita, S. Irisawa, H. Akamatsu, K. Sakashita, O. Morikawa, H. Konishi, Tetrahedron 54 (1998) 2691;
(e) N.A. Van Draanen, S. Arseniyadis, M.T. Crimmins, C.H. Heathcock, J. Org. Chem. 56 (1991) 2499.
[2] Y. Kondo, A. Yoshida, T. Sakamoto, J. Chem. Soc. Perkin Trans. 1 (1996) 2331.
[3] K.A. Swiss, C. Woo-Baeg, D.C. Liotta, A.F. Abdel-Maryanoff, J. Org. Chem. 56 (1991) 5978.
[4] J.F. Allen, K.W. Henderson, A.R. Kennedy, J. Chem. Soc., Chem. Commun. (1997) 1149.
[5] (a) K.W. Herdon, R.E. Mulvey, A.E. Dorigo, J. Organomet. Chem. 518 (1996) 139;
(b) K.W. Herdon, R.E. Mulvey, W. Clegg, P.A. O'Neil, J. Organomet. Chem. 237 (1992) 250.
[6] $MgEt_2$ reacting with HC = C^{t}Bu (1:2 molar ratio) in THF yields compound **10** directly. ^{1}H-NMR (300 MHz, C_6D_6) for **10**: δ 1.32 [s, 18H, $C(CH_3)_3$], 1.42 (m, 16H, 3, 4-thf–H), 3.79 (m, 16H, 2, 5-thf–H).
[7] N. Kuhn, M. Schuiten, J. Organomet. Chem. 421 (1991) 1.
[8] D.V. Armstrong, K.W. Henderson, M. MacGregor, R.E. Mulvey, M.J. Ross, W. Clegg, P.A. O'Neil, J. Organomet. Chem. 486 (1995) 79.
[9] M.M. Olmstead, W.J. Grigsby, D.R. Chacon, T. Hascall, P.P. Power, Inorg. Chim. Acta 251 (1996) 273.
[10] W. Clegg, F.J. Craig, K.W. Henderson, A.R. Kennedy, R.E. Mulvey, P.A. O'Neil, D. Reed, Inorg. Chem. 36 (1997) 6238.
[11] (a) W.S. Rees Jr, H.A. Luten, O. Just, Chem. Commun. (2000) 735;
(b) J.L. Sebestl, T.T. Nadasdi, M.J. Heeg, C.H. Winter, Inorg. Chem. 37 (1998) 1289;

(c) L.M. Englehardt, P.C. Junk, W.C. Patalinghug, R.E. Sue, C.L. Raston, B.W. Skelton, H. White, J. Chem. Soc., Chem. Commun. (1991) 930.

[12] (a) K.W. Henderson, R.E. Mulvey, J. Organomet. Chem. 439 (1992) 237;
(b) D.R. Armstrong, W. Clegg, R.E. Mulvey, R.B. Rowlings, J. Chem. Dalton Trans. (2001) 409;
(c) M. Westerhausen, W.Z. Schwartz, Anorg. Allg. Chem. 609 (1992) 39;
(d) L.M. Engelhardt, B.S. Jolly, P.C. Junk, C.L. Raston, B.W. Skelton, A.H. White, Aust. J. Chem. 39 (1986) 1337.

[13] B. Schubert, U. Behrens, E. Weiss, Chem. Ber. 114 (1981) 2640.

[14] T.Y. Her, C.C. Chang, G.H. Lee, S.M. Peng, Y. Wang, Inorg. Chem. 33 (1994) 99.

[15] P.J. Bailey, C.M.E. Dick, S. Fabre, S. Parson, J. Chem. Dalton Trans. (2000) 1655.

[16] R.A. Bartlett, M.M. Olmstead, P.P. Power, Inorg. Chem. 33 (1994) 4800.

[17] J.F. Allen, W. Clegg, K.W. Henderson, L. Horsburgh, A.R. Kennedy, J. Organomet. Chem. 559 (1998) 173.

[18] P.R. Markies, O.S. Akkerman, F. Bickelhaupt, W.J.J. Smeets, A.L. Spek, Adv. Organomet. Chem. 32 (1991) 147.

[19] C.C. Chang, B. Srinivas, M.L. Wu, W.H. Chiang, M.Y. Chiang, C.S. Hsiung, Organometallics 14 (1995) 5150.

[20] M. Geissler, J. Kopf, E. Weiss, Chem. Ber. 122 (1989) 1395.

[21] N.A. Bell, I.W. Nowell, H.M.M.Shearer, J. Chem. Soc., Chem. Commun. (1982) 147.

[22] (a) L.J. Guggenberger, R.E. Rundle, J. Am. Chem. Soc. 86 (1964) 5344;
(b) G. Stucky, R.E. Rundle, J. Am. Chem. Soc. 85 (1963) 1002;
(c) E. Weiss, J. Organomet. Chem. 4 (1965) 101;
(d) G.E. Coates, D. Ridely, J. Chem. Soc. A (1967) 56.

[23] E.J. Gabe, F.L. Lee, Y. Le Page, in: G.M. Sheldrick, C. Krüger, R. Goddard (Eds.), Crystallographic Computing 3; Data Collection Structure Determination, Protein, and Databases, Clarendon Press, Oxford, UK, 1985, p. 167.